Local Atomic Structure of Partially Ordered NiMn in NiMn/NiFe Exchange-Coupled Layers: 2. Electronic Structure Calculations

Angel J. Garcia-Adeva,[†,||] Rafael C. Howell,[†] Steven D. Conradson,*[,†] Jose F. Mustre de Leon,[‡] and Francisco J. Espinosa-Faller[§]

Materials Science and Technology Division, Los Alamos National Laboratory, Los Alamos, New Mexico 87545, CINVESTAV, Universidad de Mérida, Mérida, Yucatán 97310, México, and Centro Marista de Estudios Superiores, Periférico Norte Tablaje 13941, Mérida, Yucatán, México

Received: November 12, 2003; In Final Form: July 14, 2004

Local electronic and magnetic structure calculations for NiMn exchange bias alloys are reported for clusters containing NiMn in both the chemically disordered face-centered cubic and the chemically and magnetically ordered $L1_0$ phases. The results of these calculations are consistent with our local structure measurements that point toward the existence of nanometer-scale ordered clusters at the beginning stages of chemical ordering. The spatial dependence of both the local density of states and the magnetization is strongly influenced by the existence of magnetic order on short length scales, giving rise to an inhomogeneous profile for these quantities across the material with the greatest change at the interface that is still small enough within the domain to imply that the magnetization is still highly developed.

Introduction

The problem of nanoscale phase separation or heterogeneity and its correlation with the poorly understood properties of many complex correlated materials is becoming more important.[1−9] In the first paper of this series of manuscripts on exchange bias layered materials,[10] we have presented experimental results describing the correlation between short range order, the tetragonal distortion, and the local magnetic structure of NiMn in films obtained by X-ray absorption fine structure (XAFS) spectroscopy. These measurements provide evidence of the existence of nanoscale ordered (magnetic) clusters at the early stages of chemical ordering, in contrast with the standard picture for this type of compounds.[11,12] Herein, we begin to address the next issue pertaining to this topic, whether the properties of domains below the diffraction limit in size that are ordered or structured differently from the average can influence the macroscopic properties. Electronic structure calculations in the framework of the linear muffin-tin orbital method with atomic sphere approximation (LMTO-ASA) for NiMn alloys in the CuAu ($L1_0$) structure indicate that the total energy of the system is minimized by an antiparallel arrangement of the Mn magnetic moments along the $\vec{c}$ axis[13] (Figure 1). This magnetic configuration gives rise to a pseudo-gap in the density of states at the Fermi level, E_F. The main problem with this picture is that it is inconsistent with our experimental results. Indeed, according to these calculations, long-range chemical order is a prerequisite for the appearance of antiferromagnetism, in contrast with our experimental findings.

The main issue then is how this picture has to be modified to accommodate the existence of measurable nanoscale AF order as a precursor of magnetic order in larger domains. This involves considering the following aspects of the problem:

1. Why is the formation of nanoscale heterogeneities energetically/entropically favored despite increased interfacial energy?

2. What is the relationship between chemical order ($L1_0$ structure) and magnetism as opposed to that of chemical disorder (face-centered cubic (FCC) structure) and nonmagnetism, i.e., what is the mechanism by which localized magnetic moments are formed in the chemically ordered phase?[14,15] Unfortunately, in this particular case, theory has lagged behind experimentation in great part due to the well-known difficulties to perform ab initio calculations in large enough systems, including electronic correlations that give rise to magnetism from first principles.

3. Assuming that the two previous points are true (as experimental evidence suggests), how does the existence of nanoscale AF clusters manifest itself on the magnetic and electronic properties of the system? It is obvious that standard approaches based on supercell calculations are no longer valid, not only due to the absence of periodicity but also because they will not include the local effects originating in small, differently ordered domains that could, for example, exhibit magnetic order when the host does not. These may have only minimal effects on properties derived from the entire, average lattice but will, if their individual properties are retained when embedded in the host, nevertheless produce observable behaviors. Therefore, a local approach is necessary to investigate the electronic and magnetic properties of this aperiodic system (and in general of any aperiodic system).

4. What are the structural implications of a system composed of two coexisting phases or structures? Why are nanoscale domains invisible to conventional crystallographic approaches but easily observed in local structure measurements such as extended X-ray absorption fine structure (EXAFS)?

Points one and two are outside the scope of the present work, even though answering the first one is a research project our group is currently pursuing. Question four is addressed in the

* Author to whom correspondence should be addressed. E-mail: conradson@lanl.gov

[†] Los Alamos National Laboratory.

[‡] Universidad de Mérida.

[§] Centro Marista de Estudios Superiores.

[||] Current affiliation: Departamento Fisica Aplicada I, Escuela Superior de Ingenieros de Bilbao, Alda. Urquijo s/n, 48013 Bilbao, Spain.

10.1021/jp0374509 CCC: $30.25
Published on Web 04/29/2005

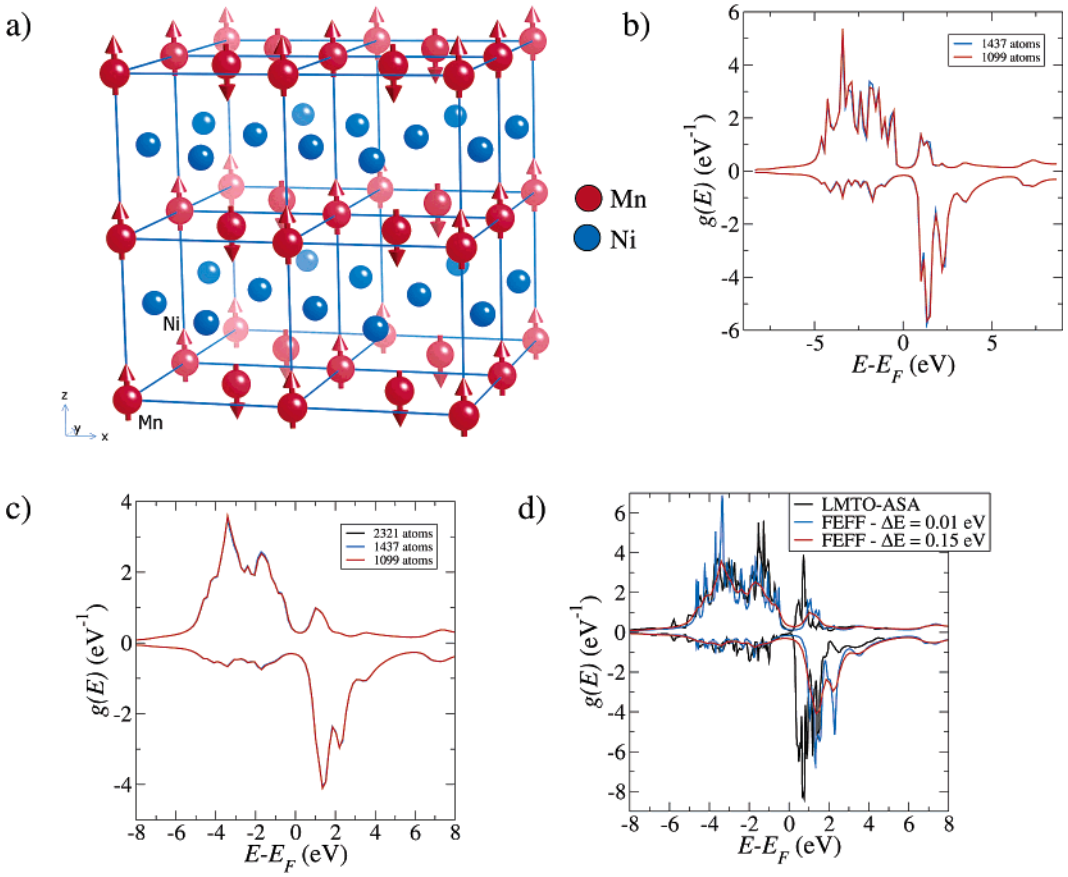

Figure 1. (a) Four unit cells of the chemically ordered ($L1_0$) NiMn compound. Lattice parameters are $a = b = 3.74$ Å and $c = 3.52$ Å. Red vectors indicate the direction of the Mn magnetic moments in the AF configuration. (b) FEFF calculated LDOS for clusters similar to the one depicted in part a with 1099 and 1437 atoms, respectively. The imaginary part of the potential (ΔE) for these calculations is 0.01 eV. (c) Same as part b for clusters containing 1099, 1437, and 2321 atoms, respectively. ΔE was set to 0.15 eV for these calculations. (d) Comparison between the LDOS calculated with FEFF (2321 atoms) and the one from the LMTO-ASA method for different values of ΔE.

first manuscript of this series. This work is concerned with answering the third point. To this end, we have conducted ab initio spin-polarized electronic structure calculations of the local density of states (LDOS) for clusters containing both NiMn in the chemically disordered FCC phase and NiMn in the chemically and magnetically ordered $L1_0$ phase. The results reported here suggest that such a system gives rise to the existence of a macroscopic AF order that reflects itself on the magnetic properties of the system, while being very different from the typical, mean-field-like, long-range AF magnetic order described in other works.

It is important to stress at this point that the existence of domains both chemically and magnetically ordered on a length scale below the diffraction limit is not a feature that is unique to the alloy considered in this work. On the contrary, it is becoming more accepted that local lattice distortions acting collectively to produce nanoscale heterogeneity and phase separation below the diffraction limit is a hallmark of complex materials[1,2] (those that exhibit complicated transformational and both electronic and atomic correlated behaviors such as, for example, solid solutions, martensites, colossal magnetoresistance compounds, or high-T_c superconductors[3−9]).

The manuscript is organized as follows. In the next section, we introduce the physical model that we will use to interpret the electronic structure including magnetic ordering of the NiMn compound. In section III, we will describe the computational method used to calculate the local electronic density of states. We will present the results of those calculations in section IV. Section V states the conclusions of this work.

Physical Model for the Magnetic Structure

On the basis of the introduction, studying the magnetic structure of these systems requires considering the existence of nanoscale magnetically ordered clusters ($L1_0$) embedded in the chemically disordered (nonmagnetic) FCC phase. The size of the chemically ordered clusters and evolution of short- into long-range order depend on the growth substrate temperature (as explained in the first paper of this series). The salient characteristics of this arrangement of atoms are that the electronic structure associated with these domains is local and derived from the arrangement of neighboring atoms in this inhomogeneous, aperiodic structure rather than being identical throughout the lattice and that the properties are determined by integrating these local ones as opposed to determining an average over a supercell. Of course, conducting electronic structure calculations for a system large enough to accommodate a statistically meaningful number of nanoscale ordered domains (of different sizes, regularly vs aperiodically distributed, etc.) is outside current computational capabilities. For that reason, we have studied simplified model systems consisting of a thick slab of NiMn in the FCC phase in which a stripe of the $L1_0$ phase (of different widths) is embedded at the center. An example of such a system can be seen in Figure 2. For clarity, we have depicted the projections along the three crystallographic axes. The FCC phase is chemically disordered while keeping the average equal composition. The atoms in the $L1_0$ stripe have antiferromagnetically aligned magnetic moments with an arrangement similar to the one described in the previous section (see also Figure

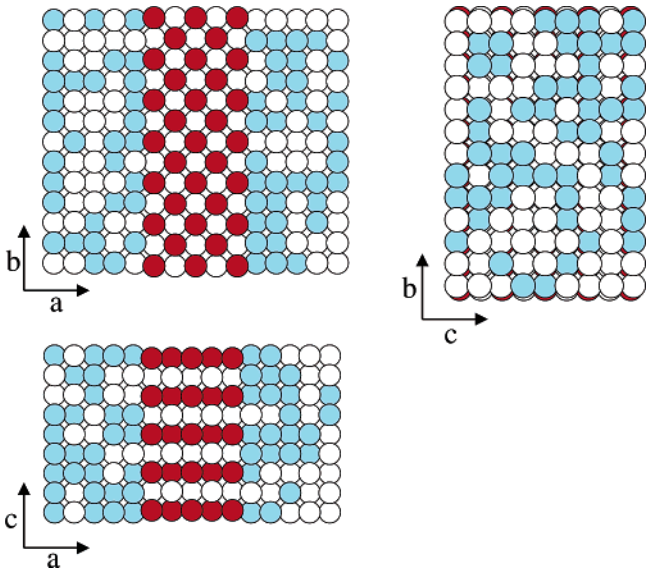

Figure 2. Example of chemically disordered FCC NiMn slab with an embedded $L1_0$ NiMn stripe. Mn atoms in the $L1_0$ phase are depicted in red. Mn atoms in the FCC phase are depicted in blue. White atoms represent Ni. The lattice parameters are $a = b = 3.74$ Å, $c = 3.52$ Å, and $a = b = c = 3.64$ Å for the FCC and $L1_0$ phases, respectively.

1a). It is important to stress some facts about this heterogeneous system. On one hand, we do not have any experimental information about the boundary between the face-centered tetragonal (FCT) and FCC phases. Therefore, we chose the simplest possible model for this interface, a boundary consisting of a single layer. This particular model minimizes the problems associated with not knowing the structure of the interface. The degree of dislocation at the interface can then be selected by the choice of the *z*-coordinate of the path along *x* that is taken through this set of atoms. Even though there are some indications that suggest that this type of abrupt boundary occurs in real alloys,[16−18] we cannot neglect the possibility that this is not the case for the NiMn alloy. An alternative description of this interface could also be a domain wall in which both distances and magnetic moments relax over several lattice distances. However, implementing such an interface would require a much bigger lattice than computationally feasible. Moreover, as we will see in section IV, our simplified model provides some hints about the relaxation mechanism (at least for the magnetic part), and therefore, we are convinced it is enough to extract some qualitative conclusions about the real system. On the other hand, someone could ask why we have chosen to describe the FCT phase as a stripe extending indefinitely in both the $\vec{b}$ and the $\vec{c}$ directions across the FCC matrix, instead of including a small cluster with finite extension in all directions. The main reason for this choice is that of computational convenience, although as an added benefit it also avoids the problem of the unknown interface structure. Indeed, this system allows us to focus on calculating the spatial dependence of the electronic properties in the $\vec{a}$ direction for the atoms located in the equatorial plane, effectively reducing our system to a one-dimensional one with respect to the spatial dependence of its electronic properties. This greatly reduces the number of different calculations we have to perform for our model system. In contrast, working with a cluster of finite extension in all the three spatial directions would necessitate paying attention to the real three-dimensional aspect of the spatial dependence of its electronic properties, with the increasing computational cost associated. Moreover, it is reasonable to expect that changes in the electronic structure due to the interface between FCT and FCC phases are more important than changes between the electronic properties of atoms located at interfaces with a slightly different environment. (In fact, even though we will not report them here, we have some preliminary results that support this fact, i.e, the change from magnetic FCT to nonmagnetic FCC induces a stronger change in the electronic properties than the one due to considering atoms located at different interfaces. This is even more likely to hold in the spherically symmetric approximation used herein.)

Method of Calculation

To calculate the spin-polarized electronic LDOS for the systems described in the previous section, we have used the ab initio self-consistent real-space code FEFF.[19,20] Its main advantages are the possibility of dealing with aperiodic systems, because it is based on a real-space approach, and it is very fast for reasonable cluster sizes ($N \approx 1000$ for the present system). There are other more sophisticated and accurate methods reported in the literature (as it is likely the case for the LMTO-ASA method used in ref 13), but they have the disadvantages of being only applicable to periodic systems and more computationally demanding. Taking into account that the present work involves more than 70 runs of the code, the running time is a decisive factor when it comes to choosing an ab initio method for our calculations. Another advantage is the fact that electronic properties calculated with FEFF are calculated locally. This is an essential feature to compare calculated electronic structure with local measurements. Besides all of the advantages of using the FEFF code mentioned above, it is also important to mention that the parallel version of this code has the invaluable feature that the CPU time involved in a particular calculation scales linearly with the inverse number of parallel processes. It would have been very difficult otherwise to conduct simulations for system sizes such as the ones investigated in this work. Calculations reported in this manuscript have been performed in the QSC cluster located at the Los Alamos National Laboratory by using the parallel MPI version of FEFF 8.2.[21] The QSC consists of 256 4-CPU HP/Compaq Alphaserver ES45 machines. Each node has 16Gb of RAM with a peak speed of 2.56 teraflops. The typical running time for one of our runs using 128 CPUs is 1.5 h. The memory used for these calculations is around 400 Mb per process. Further details about the use of the FEFF code and the theory behind it can be found in refs 19, 20, and 21. Details about the parallel implementation of FEFF can be found in ref 22. A discussion about spin-dependent calculations of X-ray absorption spectra can be found in refs 23 and 24. Finally, links to real-world examples of FEFF calculations can be found at the FEFF project webpage.[25]

Electronic LDOS were calculated for clusters of chemically disordered FCC NiMn in which stripes of the chemically and magnetically ordered $L1_0$ phase of different widths were embedded. The width of these stripes ranges from six to nine atomic layers (Figures 3a−7a). We have focused on magnetic stripes with an odd number of atomic layers because this allows us to reduce the number of unique sites (unique potentials in the FEFF terminology) entering in the LDOS calculation by a factor of 2. The only exception to this rule is a stripe with a width of six atomic layers that was used to check whether the results depend on the parity of the stripe width. The Mn atoms inside the FCT stripe possess magnetic moments that define a spin configuration similar to the one depicted in Figure 1. The atoms outside the FCT stripe do not possess a magnetic moment, and they are chemically disordered and exhibit a spatial

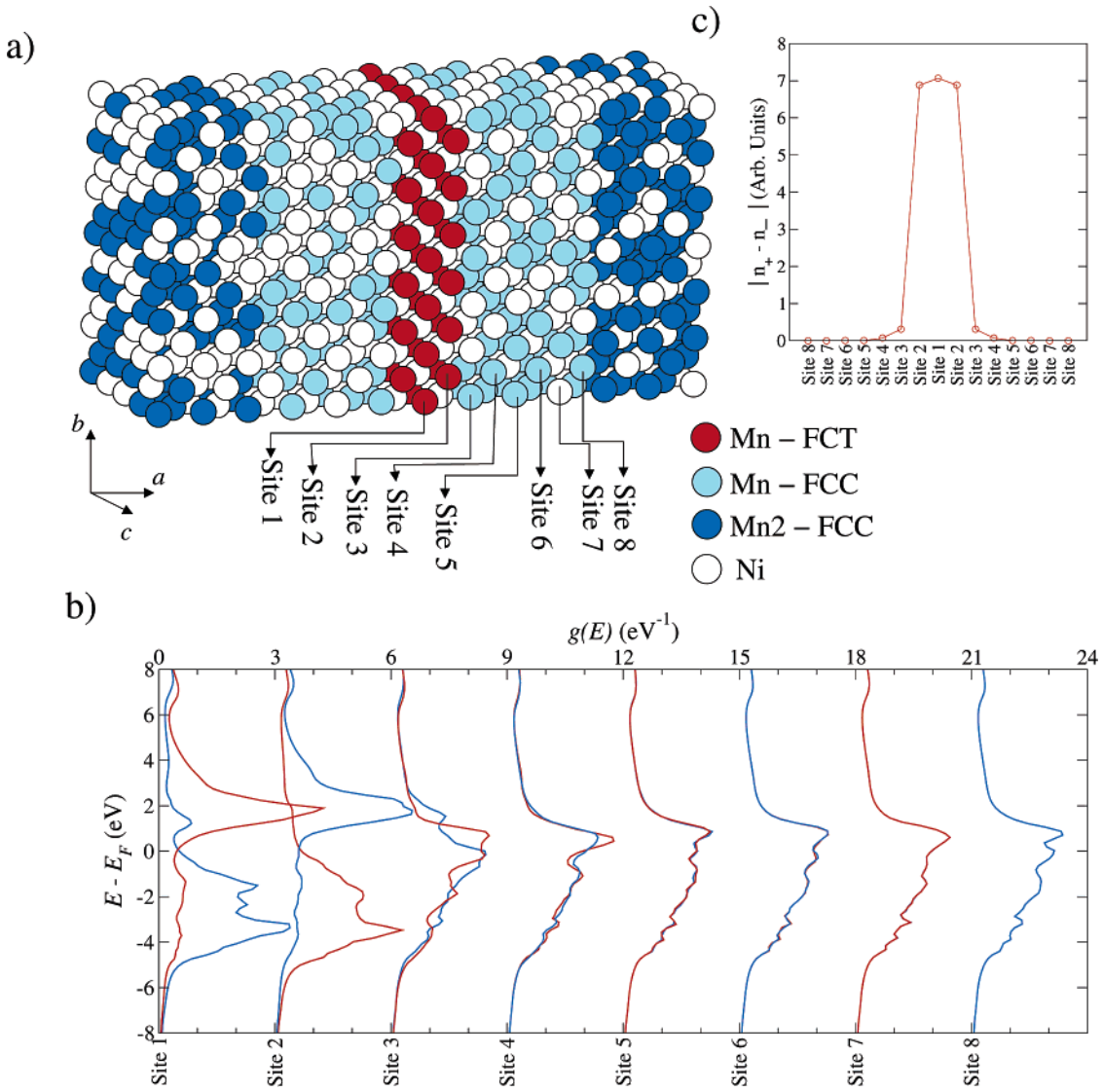

Figure 3. (a) NiMn cluster with a stripe of FCT NiMn of three atomic layers in width at the center. The different unique sites used for the LDOS calculation are indicated. Dark blue atoms represent extra Mn atoms added to the system to ensure convergence of the SC calculations. They are represented by a single unique potential in FEFF. (b) LDOS for the Mn atoms for the different sites depicted in part a. Blue curves represent up-spin configuration of the Mn atoms at site 1. Red curves represent down-spin configuration of the Mn atoms at site 1. (c) Magnetization profile at $T = 0$ K for the cluster in part a.

arrangement with cubic symmetry. The reason various different widths were considered is our lack of knowledge about the exact size of the nanoscale magnetic clusters present in the NiMn system. We expected that calculations for different stripe widths would provide some information about this point and, at the same time, information about the minimum size required for the antiferromagnetism to be expressed by the atoms within the embedded domain. For this reason, the calculations were limited to the Mn atoms. Two criteria for evaluating the extent to which the properties inherent to the minority component of the heterogeneous structure are evident. The difference between the amount of up- and down-spin at a given site provides a quantitative measure, albeit subject to the limitations of the calculation methodology used. Other characteristics of the LDOS that can be associated with the antiferromagnetism, i.e., the gap across the Fermi level, are more difficult to interpret but may provide a better indication of the trends that occur across the probed line of atoms.

The size of the system was chosen trying to maintain a compromise between resolution of the calculated LDOS and speed. Fortunately, due to the self-consistent (SC) character of the algorithms used by FEFF, relatively small clusters provide well-converged results. To avoid boundary effects in the SC part of the calculation (which only takes into account those atoms located around a small sphere centered at the absorber atom), additional atoms in the FCC phase where added at the borders of our clusters to ensure that all the SC spheres around the absorber atom contained the same number of atoms (Figure 3a). These extra atoms were characterized by a single unique potential, and its LDOS is not reported. Including these extra atoms, the total number of atoms in our clusters adds up to 1463 (i.e., a cluster containing $25 \times 13 \times 9$ atomic layers along the three crystallographic directions, respectively) for the odd-width stripes and 1521 (i.e., a cluster containing $26 \times 13 \times 9$ atomic layers along the three crystallographic directions, respectively) for the cluster with a stripe width of six atomic layers. The finite size of the clusters imposes a resolution limit to the calculated LDOS that is related to the electron mean free path. This reflects on the finite (Lorentzian) width of the LDOS peaks. To estimate the value of this finite size broadening, we used the following approach. Three purely periodic, FCT NiMn clusters containing 1099 ($13 \times 13 \times 13$ atomic layers), 1437

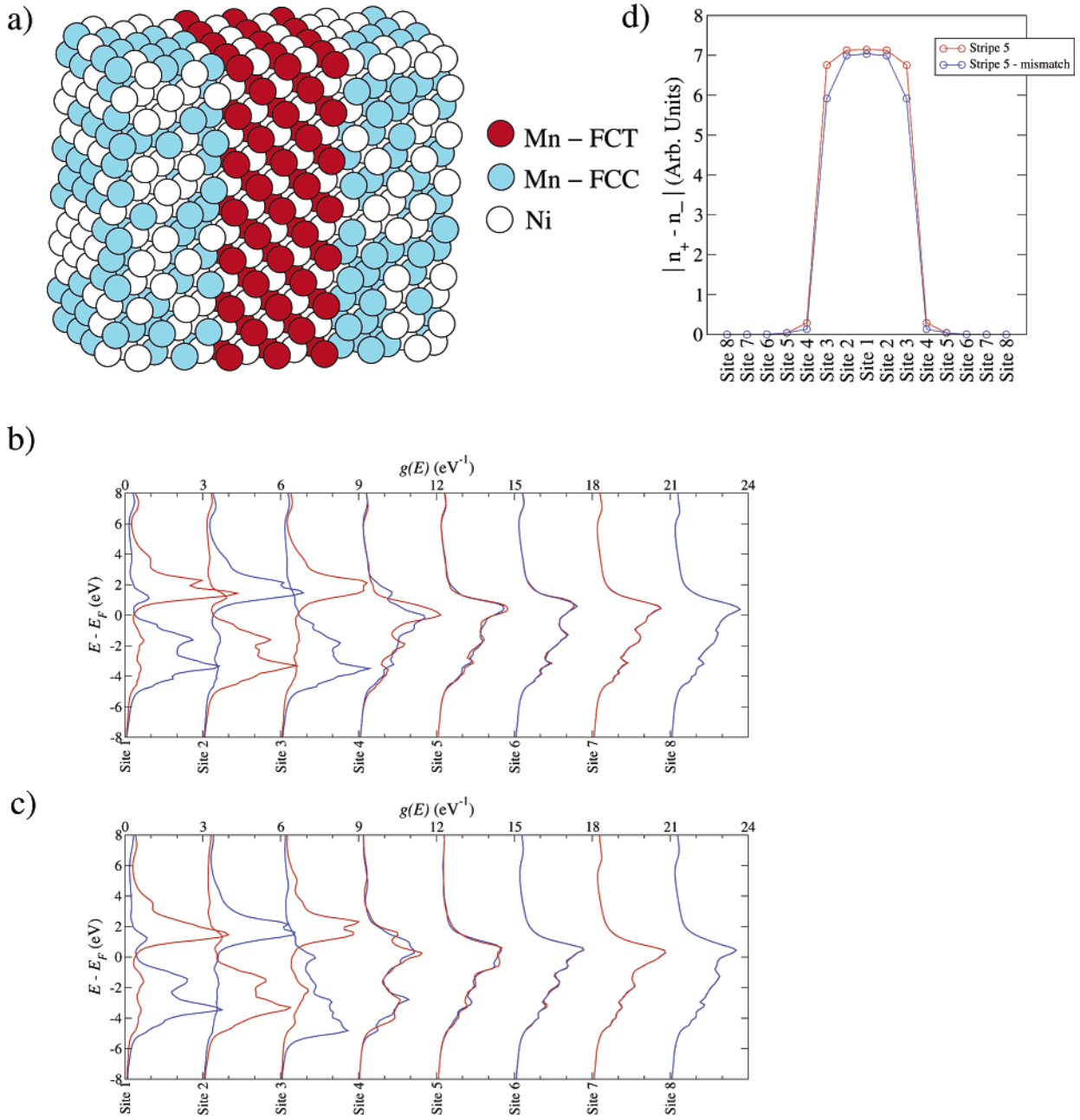

Figure 4. (a) NiMn cluster with a stripe of FCT NiMn of five atomic layers in width at the center. (b) LDOS for the Mn atoms for the different sites depicted in part a. (c) LDOS for the mismatched cluster described in the text. (d) Magnetization profile at $T = 0$ K for the cluster in part a. Blue line corresponds to the mismatched system described in the text.

($17 \times 13 \times 13$ atomic layers), and 2321 ($21 \times 17 \times 13$ atomic layers) atoms were constructed. The up and down LDOS were calculated for these clusters using different values of the LDOS broadening (ΔE) ranging from 0.01 to 0.15 eV. Some representative results are depicted in Figures 1a and 1b. It was found that the LDOS did not exhibit any size dependence for $\Delta E >$ 0.1 eV. To be on the safe side, a $\Delta E = 0.15$ eV was used for the rest of the calculations. This convergence study for the FCT system also gives us the opportunity to estimate the accuracy of our FEFF calculations when compared with other, more sophisticated methods. Indeed, a comparison between our FEFF calculations and the LMTO-ASA results of ref 13 is depicted in Figure 5d for two different values of ΔE. The pseudo-gap at E_F is fairly well-reproduced by our calculations. Moreover, even the fine structure of the LDOS can be accurately reproduced by using a small value of ΔE. However, for the reasons explained above, we will use a larger value of ΔE for the rest of calculations. Besides, it is obvious that the value of ΔE does not affect the calculated magnetization, which is the physical quantity we are most interested in. There are, however, some quantitative differences between the LDOS calculated by both methods. In particular, the peaks above E_F are shifted toward higher energies in our calculations by $\sim$1 eV. Also, below E_F, the largest LDOS occurs around -3 eV, whereas for the LMTO calculations the largest LDOS occurs closer to E_F. These differences can be traced to different exchange correlation potentials used by these methods. In any case, we think it is fair to say that FEFF does a very good job reproducing the qualitative features of the LMTO LDOS while being faster and applicable to aperiodic systems.

Regarding the particular parameters used for the LDOS calculations, a radius of 9.3 Å was used for the full multiple scattering (FMS) calculation. For the self-consistent part, a radius of 5.3 Å was chosen to include five coordination shells

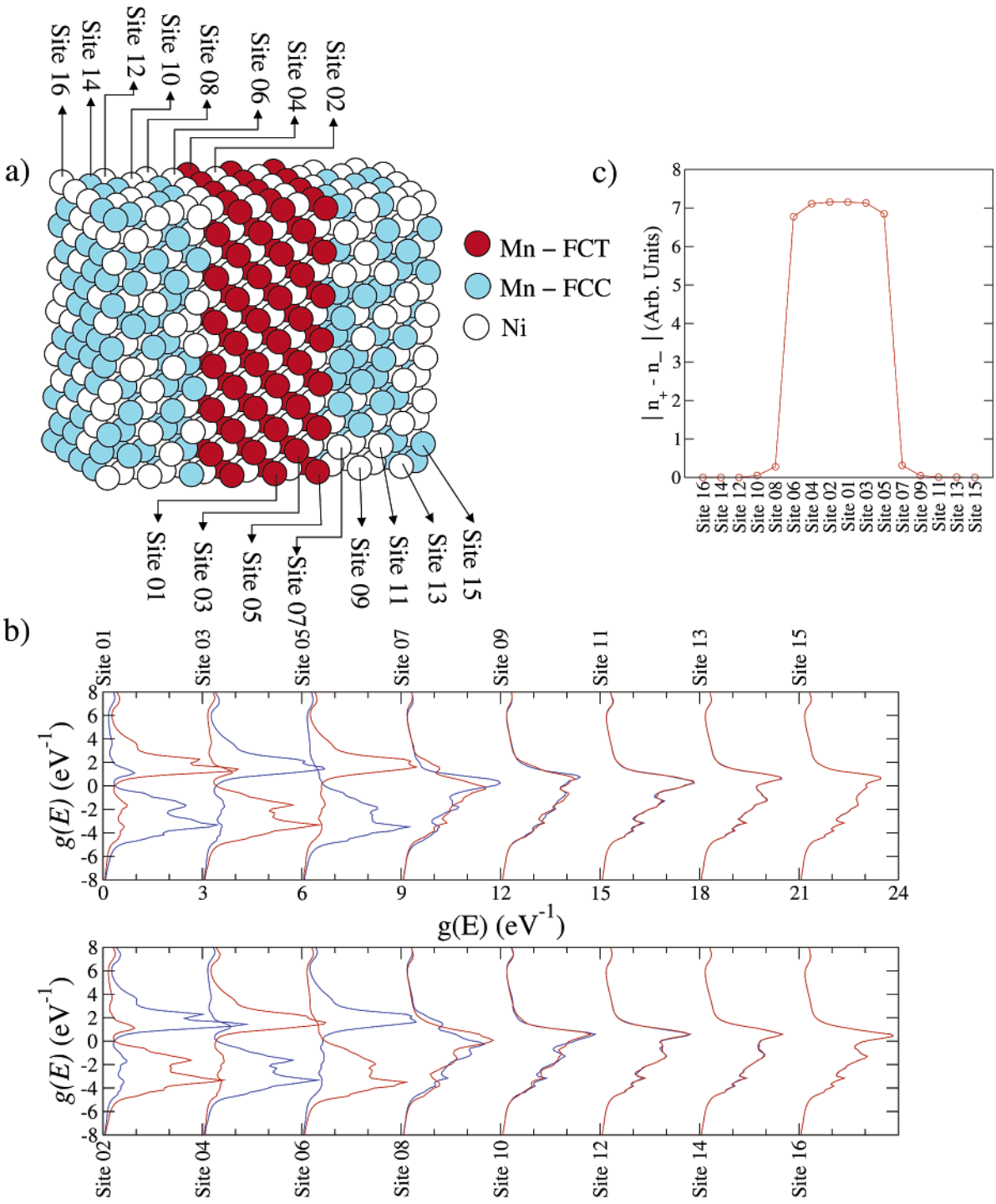

Figure 5. (a) NiMn cluster with a stripe of FCT NiMn of six atomic layers in width at the center. The different unique sites used for the LDOS calculation are indicated. (b) LDOS for the Mn atoms for the different sites depicted in part a. (c) Magnetization profile at $T = 0$ K for the cluster in part a.

in the SC sphere. A convergence acceleration factor of 0.05 was used for the Broyden algorithm. Before starting the Broyden algorithm, 10 mixing iterations were done to ensure convergence. Typically, convergence in the determination of E_F was reached after 11 SC iterations. For the LDOS calculation, 11 unique sites (potentials) were used. The first 8 unique potentials correspond to Mn atoms, as depicted in Figure 3a. Potential 9 was reserved for the extra Mn atoms added to ensure convergence (the ones depicted in dark blue in Figure 3a). Potentials 10 and 11 correspond to Ni atoms. An exception to this is the stripe with six atomic layers width. For this system, due to the lack of mirror symmetry, it is necessary to use more unique potentials, up to a total of 19, as depicted in Figure 5a. Finally, the NOHOLE card was used for all of the reported calculations to simulate the effect of complete core−hole screening.

Let us now review the main results from these calculations.

Results and Discussion

The results of the LDOS calculations for NiMn clusters containing stripes of the $L1_0$ phase of different widths are depicted in Figures 3b−7b. Because the objective is to elucidate the magnetism, we only report the LDOS corresponding to the Mn atoms that exhibit the unpaired spin and not the Ni. The

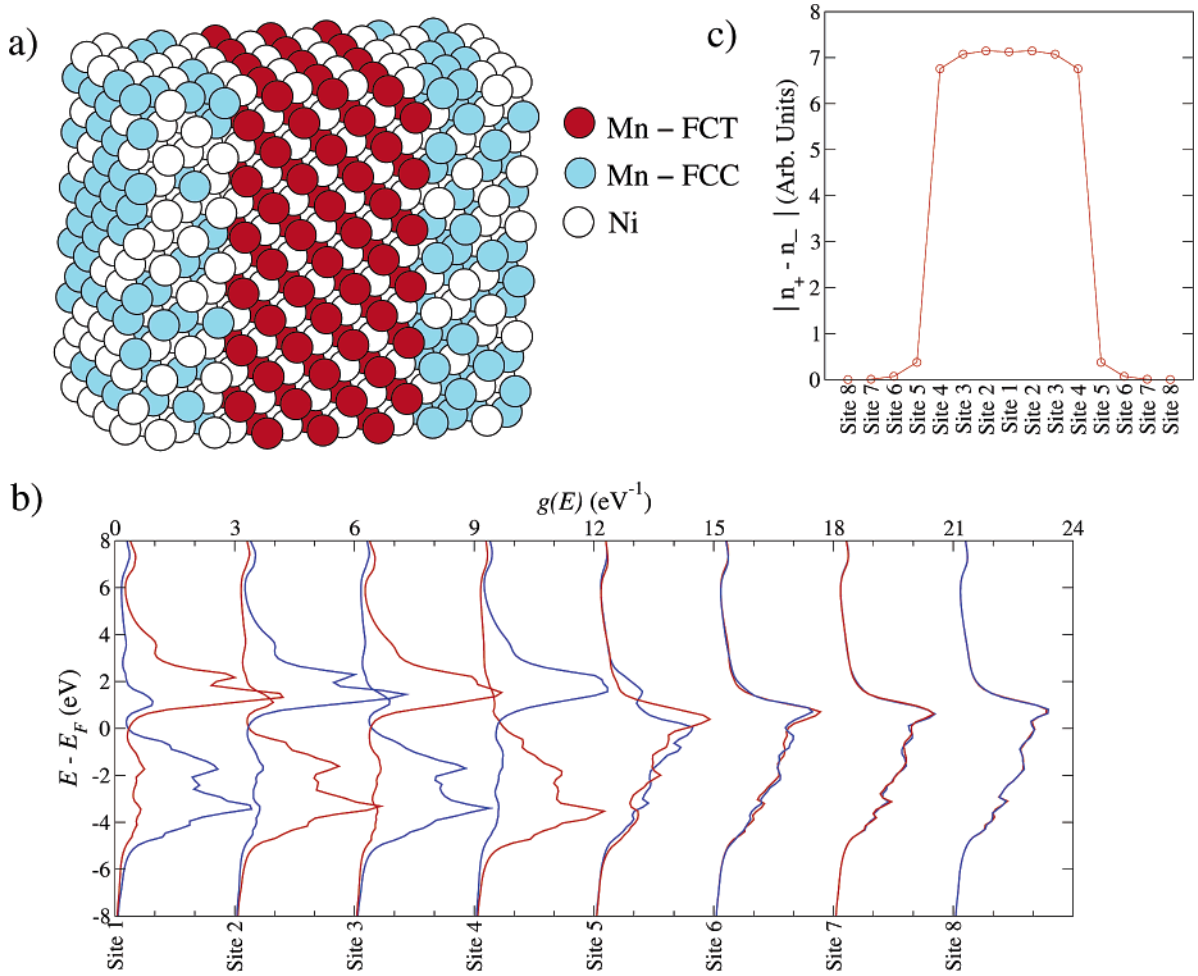

Figure 6. (a) NiMn cluster with a stripe of FCT NiMn of seven atomic layers in width at the center. (b) LDOS for the Mn atoms for the different sites depicted in part a. (c) Magnetization profile at $T = 0$ K for the cluster in part a.

positive (negative) curve stands for up-spin (down-spin) polarization.

The first interesting feature that we can notice from those figures is the similarity between the LDOS for different stripe widths. This seems to imply that the electronic properties of these systems are more sensitive to the presence or absence of localized magnetic moments rather than the particular structural details, even though these are also noticeable, as we will see below. Furthermore, the spatial dependence of the calculated LDOS is totally consistent with the intuitive idea we can extract from our physical model, namely, the existence of a pseudo-gap at E_F inside the FCT stripe and a large shift of the densities of states for up and down polarizations. Outside the magnetic stripe, the gap disappears as well as the asymmetry between the up and down densities of states. Actually, we must point out that the pseudo-gap is not completely formed in the calculated LDOS, i.e., the density of states is not really zero at E_F. This is mainly due to the finite size of the clusters considered in this work and, in general, a feature of all ab initio calculations in real space that can only deal with a finite number of atoms.

The behavior of the LDOS at the interface between the FCT/FCC phases deserves special consideration. The asymmetry between the down and up LDOS does not disappear suddenly at the boundary of the magnetic stripe, but even outside the FCT stripe the LDOS exhibits a certain amount of asymmetry that falls off as we move away from the magnetic stripe. This will have important consequences on the magnetization profile as we will discuss below. It is important to notice too that, in contrast with the asymmetry of the LDOS, the pseudo-gap disappears very suddenly for our model systems. Actually, even inside the magnetic stripe, it is almost indiscernible for sites at the boundary. This has the important implication that even in the absence of the pseudo-gap there are still AF correlations present in the system. The fact that this behavior occurs irrespective of the stripe width or structural details (as can be easily seen for the mismatched stripe discussed below, see Figure 4b) seems to indicate that this is a generic property of the interface between the two phases. Furthermore, the most important changes in the LDOS are localized around the layers that constitute the interface, indicating that nearest-neighbor interactions dominate the electronic structure in this particular alloy. It would be interesting to investigate the spatial dependence of the pseudo-gap for an extended domain wall, but such a study is outside the scope of this work.

It is also important to notice that this kind of behavior (existence of AF correlations even in the absence of the pseudo-gap) has been consistently observed in high-T_c superconductors and layered manganites. In the former, the existence of the pseudo-gap is the precursor of the superconducting gap.[26] In the latter, it is the precursor of a charge-ordered state.[27] Even though the origin of this effect is still under discussion, one scenario that is becoming widely accepted is that of phase separation on the nanoscale.[6,7] It is, thus, quite interesting to observe that analogous effects occur in our model systems and that these are clearly related to the existence of phase separation below the diffraction limit.

As mentioned in the previous section, we also conducted LDOS calculations for a stripe with a width of six atomic layers

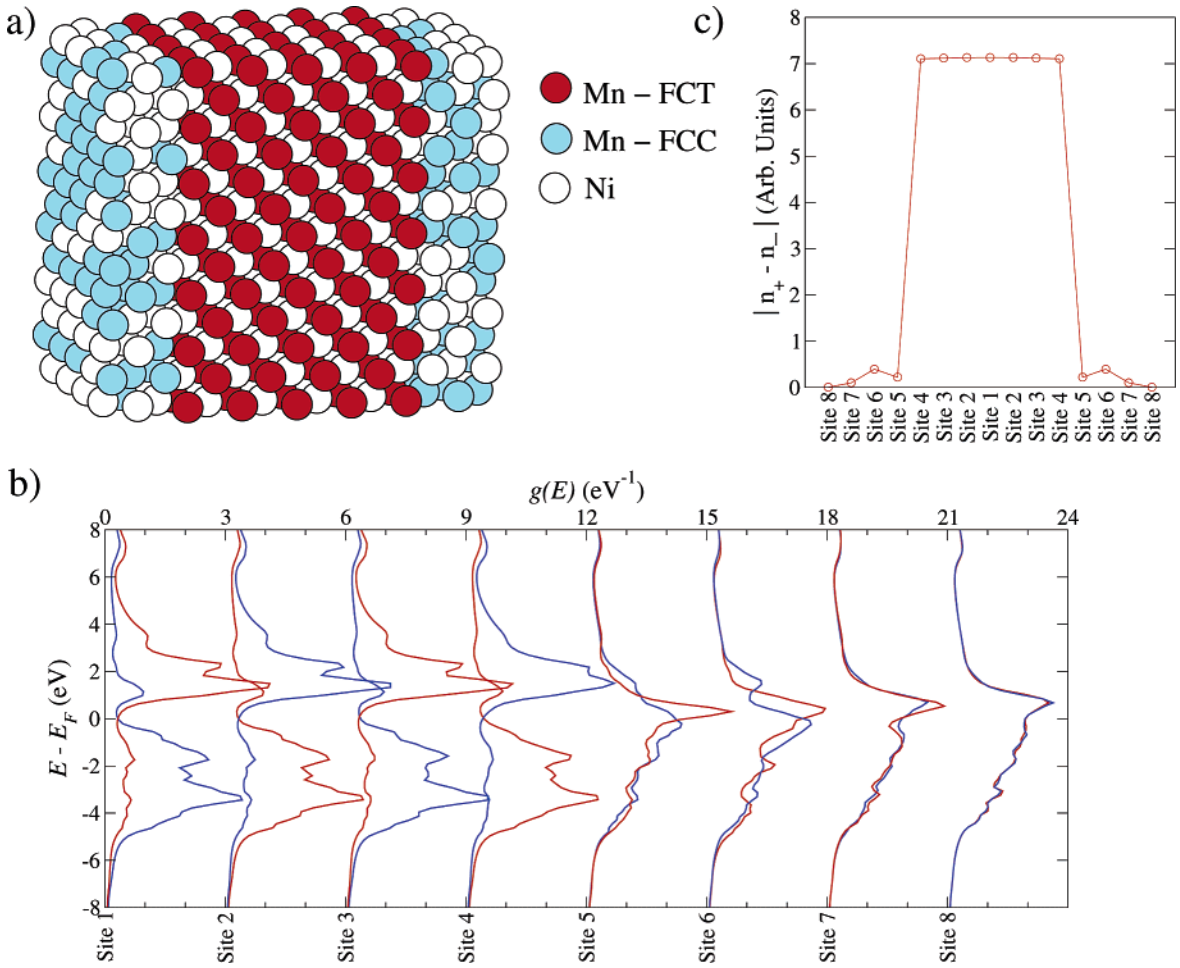

Figure 7. (a) NiMn cluster with a stripe of FCT NiMn of nine atomic layers in width at the center. (b) LDOS for the Mn atoms for the different sites depicted in part a. (c) Magnetization profile at $T = 0$ K for the cluster in part a.

to check whether any of the features depend on the parity of the stripe. The results are depicted in Figure 5b. As it is easy to see, there are some very small differences between the LDOS for sites labeled with an odd number (used for sites located on the right half of the cluster) and the equivalent even site. However, these differences are almost negligible when compared with the ones occurring across the magnetic stripe. Therefore, it seems justified to say that electronic properties do not greatly depend on the parity of the magnetic stripes, as expected.

There is another important aspect of our calculations that must be checked for consistency. The present clusters have been constructed in such a way that the central *ac* plane of the $L1_0$ stripe exactly coincides with the central *ac* plane of the rest of the atoms in the FCC phase. In other words, assuming that the atoms in the central layer of the FCT stripe are located at (0, 0, 0) positions relative to the unit cell (plus symmetry operations), the atoms in the next layer are located at (0.5, 0.5, 0) positions, and this relation holds even as we move across the FCT/FCC boundary. However, as we can easily see in Figure 2, this is not the case as we move along the $\vec{c}$ axis, due to the incommensurability of the lattice parameters for both phases. This implies that for these infinitely long stripes the relative placement of the two layers at the boundary shifts as we move along the $\vec{c}$ axis. In fact, for some other *ac* plane of an ideally infinite cluster, this shift can even amount to one-half of the FCC lattice parameter, so when we move across the FCC/FCT boundary, the atoms in both layers are occupying the (0, 0, 0) positions. Obviously, it is extremely important to assess how this incommensurability affects the LDOS to check if our calculations are representative of the whole system. Of course, doing an exhaustive analysis of this issue would imply studying the spatial dependence of the LDOS along the $\vec{c}$ axis (and also along the $\vec{b}$ axis). However, as we mentioned above, this would greatly increase the number of required computations, making it impractical. Therefore, we performed a single calculation for the most extreme case of lattice mismatch that involves a shift of one-half of the FCC lattice parameter. We can expect this particular configuration to exhibit the largest deviations with respect to the rest of calculations reported in this work. The resulting LDOS is depicted in Figure 4c. As we can see, there are noticeable differences between both LDOS, especially for the layers located at the boundary, as expected. The pseudogap at site 2 is shallower for the mismatched stripe. The up-spin LDOS for site 3 is shifted toward lower energies below E_F. Finally, the LDOS exhibits a noticeable dip below E_F for site 4. The LDOS is quite similar for the rest of sites. In any case, these qualitative differences are still less important than the ones due to the presence/absence of magnetic moments. Besides, it is obvious that these types of effects are exaggerated in our simplified model. For small FCT clusters, finite in the three spatial directions, only small deviations with respect to perfect matching between the layers would be possible, giving rise to very small variations of the LDOS for different sites at the different interfaces. Similar calculations have been performed for the other stripes. The results are quite similar to this example, and we will not report them here.

An interesting physical quantity for the present problem can be calculated once we have the LDOS is the magnetization at

$T = 0$ K. This quantity is easily calculated by numerical integration of the LDOS

$$m \approx \int_{-\infty}^{E_F} (g_\uparrow(E) - g_\downarrow(E))\, dE \quad (1)$$

where $g_\uparrow(E)$ ($g_\downarrow(E)$) stands for the up-spin (down-spin) LDOS. The results for the absolute value of this quantity are depicted in Figures 3c−7c. It can be seen that this quantity exhibits a profile totally consistent with the proposed physical model. For each individual layer inside the magnetic stripe, there is a net magnetization, and its magnitude falls to zero as we cross the boundary into the nonmagnetic region. It is interesting to notice, however, that it does not fall to zero suddenly at the boundary between the FCT and FCC phases, but instead, the decay of m starts inside the magnetic stripe, at the boundary, and it is nonzero for the boundary layer in the FCC phase. In turn, this suggests that for an extended boundary the magnetization would exhibit a tail outside the magnetic cluster and inside the nonmagnetic region. The only exception to this behavior occurs for the stripe consisting of nine atomic layers. In this case, the magnetization is constant inside the magnetic stripe, except for the atoms at the boundary with the $L1_0$ phase, and there is a small ripple in the nonmagnetic layer. The flatness of the magnetization inside the stripe is consistent with the fact that we are approaching the limit in which the whole solid is in the $L1_0$ magnetic phase and a long-range magnetic order is expected. However, we do not have an explanation at this point for the ripple occurring outside the magnetic phase. It is easy to trace this unexpected behavior to the qualitative features of the LDOS for this particular system. Indeed, as can be seen in Figure 7b, the LDOS for site 5 is qualitatively different from the rest of the LDOS for other stripe widths. In fact, it looks more similar to the LDOS in the FCC phase. As mentioned above, we cannot state at this point whether this is an artifact of our calculations or if it has real physical meaning. In any case, the change in the magnetization across the interface is obviously much smaller than the observed change in the LDOS. We believe that, although the trend is correct, it is likely that the perturbation of the magnetization would actually be much larger and the evolution from the properties inherent to the two structures more gradual. This exemplifies our opinion that, in compromising between speed and accuracy for the large number of calculations needed for this work, the patterns found by faster calculation methods will be valid even when the actual values they determine are only partly so. Slower, more accurate calculation methods may then be used to correct them.

There is another interesting aspect related to the spatial dependence of the magnetization. For odd-width stripes, the net magnetization of the stripe is nonzero (if we take the sign into account). This is, of course, no longer true for a real material where we have a statistical distribution of nanoscale magnetic domains and some of them equilibrate the net magnetization of other domains. Still, it is interesting to point this out because this situation is inherent to the characteristic size (3−4 cells) of the magnetic clusters involved in this problem and it is radically different from the situation in standard long-range AF materials. As we can also see from Figure 5c, for even-width stripes, the net magnetization of the whole cluster is exactly zero, even though the LDOS for different sites were calculated independently for each site (incidentally, this provides an additional consistency check for the FEFF calculations).

Conclusions

The results reported in this work for both the electronic local density of states and the magnetization profile in the NiMn exchange bias alloy provide a representative picture of how these properties are modified by the existence of magnetically and chemically ordered nanoscale clusters. For the particular system considered in this work, this picture is radically different from the standard model in which the order parameters (the staggered magnetization and chemical order) of the system are homogeneous quantities across the material. This standard description is inconsistent with our experimental findings. In contrast, a picture more consistent with our experimental results is provided by assuming that the order parameters of the system are inhomogeneous and they typically vary on the length scale below the diffraction limit, i.e., 1−2 nm. The calculated LDOS and magnetization profiles for a simple physical model of these nanoscale clusters are fully consistent with this idea and provide some clues about the relation between physical quantities affecting different length scales. It is also important to notice that this picture is not a unique feature of the type of magnetic alloys considered in this work, but it is becoming more accepted that this type of scenario involving inhomogeneous order parameters and phase separation/heterogeneity on very short length scales is relevant to a wide range of materials, usually termed complex materials, that include systems that are very important from the point of view of their technological applications, such as is the case, for example, of transformational compounds, colossal magnetoresistance compounds, or high-T_c superconductors. The behavior of the local density of states and magnetization at the interface are among the most interesting features emerging from our calculations. It turns out that the layer in the FCC phase defining this interface has certain magnetic character even though there is no pseudo-gap present. This fact has profound implications not only for the alloy considered in this work but also for other complex materials, as pointed out in section IV. Moreover, the antiferromagnetic fluctuations and pseudo-gap evolution in the magnetic stripe and across the interface are very robust against structural details as can be seen from the study of a completely mismatched interface considered above.

Another important aspect of the present calculations is related to the computational method itself. We have demonstrated its reliability when compared with other electronic structure codes based on supercell calculations, even for not too large clusters. Furthermore, FEFF has the advantage of being able to deal with aperiodic structures, because it is based on real-space calculations, it is not as computationally expensive as those other methods, and it is portable to a number of different hardware platforms. Additionally, we think that the simulations reported in this work for our heterogeneous magnetic systems constitute an example of the usefulness of this code to accurately calculate the electronic and the magnetic properties of heterostructures and interfaces.

Acknowledgment. We would like to thank Professors John Rehr and Bob Albers for several invaluable comments and suggestions about the FEFF calculations reported in this work. This work has been supported by the Department of Energy Defense Programs and Office of Basic Energy Sciences division of Chemical Sciences under Contract No. W-7405.

References and Notes

(1) Conradson, S. D. *Appl. Spectrosc.* **1998**, *52*, A252.

(2) Conradson, S. D.; Espinosa, E. J.; Henderson, A.; Villella, P. M. In *Physics in Local Lattice Distortions*; AIP Conference Proceedings 554; Oyanagi, H., Bianconi, A., Eds.; American Institute of Physics: Melville, NY, 2001; p 503.

(3) Ice, G. E.; Sparks, C. J. *Annu. Rev. Mater. Sci.* **1999**, *29*, 25.

(4) Xu, Z. A.; Ong, N. P.; Wang, Y.; Kakeshita, T.; Uchida, S. *Nature* **2000**, *406*, 486.
(5) Zaanen, J.; *Nature* **2000**, *404*, 714.
(6) Moreo, A.; Yunoki, S.; Dagotto, E. *Science* **1999**, *283*, 2034.
(7) Dagotto, E.; Hotta, T.; Moreo, A. *Phys. Rep.* **2001**, *344*, 1.
(8) Tranquada, J. M.; Sternlieb, B. J.; Axe, J. D.; Nakamura, Y.; Uchida, S. *Nature* **1995**, *375*, 561.
(9) Tranquada, J. M.; Nakajima, K.; Braden, M.; Pintschovius, L.; McQueeney, R. J. *Phys. Rev. Lett.* **2002**, *88*, 075505.
(10) Espinosa-Faller, F. J.; Howell, R. C.; Garcia-Adeva, A. J.; Conradson, S. D.; Ignatov, A. Y.; Tyson, T. A.; Farrow, R. F. C.; Toney, M. F. *J. Phys. Chem. B* **2005**, *109*, 10406.
(11) Schulthess, T. C.; Butler, W. H. *J. Appl. Phys.* **1998**, *83*, 7225.
(12) Pal, L.; Kren, E.; Kadar, G.; Szabo, P.; Tamoczi, T. *J. Appl. Phys.* **1968**, *39*, 538.
(13) Sakuma, A. *J. Magn. Magn. Mater.* **1998**, *187*, 105.
(14) Nakamura, K.; Kim, M.; Freeman, A. J.; Zhong, L.; Fernandez-de-Castro, J. *IEEE Trans. Magn.* **2000**, *36*, 3269.
(15) Kulkova, S. E.; Egorushkin, V. E. *Mater. Sci. Eng.* **1999**, *A273*−*275*, 170.
(16) Schirmer, B.; Wuttig, M. *Surf. Sci.* **1998**, *399*, 70.
(17) Kuch, W.; Parkin, S. S. P. *J. Magn. Magn. Mater.* **1998**, *184*, 127.
(18) Kusar, N.; Conradson, S. D. Unpublished work.
(19) Rehr, J. J.; Albers, R. C. *Rev. Mod. Phys.* **2000**, *72*, 621.
(20) Ankudinov, A. L.; Ravel, B.; Rehr, J. J.; Conradson, S. D. *Phys. Rev. B* **1998**, *58*, 7565.
(21) Ankudinov, A. L.; Rehr, J. J. *Phys. Rev. B* **2000**, *62*, 2437.
(22) Ankudinov, A. L.; Bouldin, C.; Rehr, J. J.; Sims, J.; Hung, H. *Phys. Rev. B* **2002**, *65*, 104107.
(23) Ankudinov, A. L.; Rehr, J. J. *Phys. Rev. B* **1997**, *56*, R1712.
(24) Ankudinov, A. L. Relativistic Spindependent X-ray Absorption Theory. Ph.D. Thesis, University of Washington, 1996.
(25) FEFF Project Home Page. http://leonardo.phys.washington.edu/feff/.
(26) Orenstein, J.; Mills, A. J. *Science* **2000**, *288*, 468.
(27) Loudon, J. C.; Mathur, N. D.; Midgley, P. A. *Nature* **2002**, *420*, 797.